



# The transition mechanisms of quantum-dot/quantum-well mixed-mode infrared photodetectors

Shih-Yen Lin<sup>a,b,c,\*</sup>, Shu-Ting Chou<sup>a</sup>, Wei-Hsun Lin<sup>d</sup>

<sup>a</sup> Research Center for Applied Sciences, Academia Sinica, Taipei 11529, Taiwan

<sup>b</sup> Department of Photonics, National Chiao-Tung University, Hsinchu 30010, Taiwan

<sup>c</sup> Institute of Optoelectronic Sciences, National Taiwan Ocean University, Keelung 20224, Taiwan

<sup>d</sup> Institute of Electronic Engineering, National Tsing Hua University, Hsinchu 30013, Taiwan

## ARTICLE INFO

### Article history:

Available online 6 June 2009

### PACS:

78.67.Hc

78.30.Fs

### Keywords:

Quantum-dot infrared photodetectors

Quantum dots

## ABSTRACT

The transition mechanisms of a 10-period quantum-dot (QD)/quantum-well (QW) mixed-mode infrared photodetector is investigated in this paper. Both mid-wavelength infrared (MWIR) and long-wavelength infrared (LWIR) responses are observed for the device. The lower normal incident absorption of the LWIR peak suggests that the QW intra-band transition is responsible for the response while the QD intra-band transition for the MWIR response. Due to the coexistence of MWIR and LWIR responses, the MWIR response should be resulted from one-photon transition while the LWIR response from the two-photon transition. To explain the transition mechanisms of the MMIP device, a model is proposed in this paper. The increases of both MWIR and LWIR responses with increasing measurement temperatures observed for the device are attributed to the increase of electrons in the QW ground state/wetting layer state resulted from the increase of one-photon absorption process with increasing temperatures.

© 2009 Elsevier B.V. All rights reserved.

## 1. Introduction

Lots of effort has been devoted to the development of quantum-dot infrared photodetectors (QDIPs) [1–6]. QDIPs with high responsivities and operation temperatures have been reported by inserting AlGaAs barrier layers [1–3]. The influence of QD doping density on the operation voltage and normal incident absorption have also been reported [4]. Device structures with p-type doped GaAs layers inserted within have been proposed [5–6]. The thermal images taken by a  $256 \times 256$  grating-less QDIP focal-plane array (FPA) operated at 135 K have also been demonstrated [7]. However, considering the thermal imaging applications of QDIPs, two major disadvantages are observed for the devices: (a) for most QDIPs, the detection wavelength is limited in the mid-wavelength infrared (MWIR, 3–5  $\mu\text{m}$ ) range and (b) the wafer uniformity of QD samples is worse than the conventional quantum-well infrared photodetectors (QWIPs). Therefore, to achieve multi-color detection at both MWIR and LWIR ranges, a 10-period QD/QW mixed-mode infrared photodetector (MMIP) is proposed in this paper. Responses at 4.8/12.7 and 5.3/10.3  $\mu\text{m}$  at positive and negative biases are observed for the device. Compared with the peaks at MWIR range, the lower normal incident absorption

of the LWIR peaks suggests that the QW intra-band transition is responsible for the responses. The QD intra-band transition should be responsible for the MWIR peaks. To explain the transition mechanisms of the device, a model is proposed. Assuming wetting layer state ( $E_{\text{WL}}$ ), QW ground state ( $E_{0,\text{QW}}$ ) and QW excited state ( $E_{1,\text{QW}}$ ) are available for the electron transition from QD excited state ( $E_{1,\text{QD}}$ ), one-photon transitions ( $E_{1,\text{QD}}-E_{\text{QW},0}$ ) and ( $E_{1,\text{QD}}-E_{\text{WL}}$ ) are responsible for the 4.8 and 5.3  $\mu\text{m}$  responses at positive and negative biases. The two-photon transitions ( $E_{0,\text{QW}}-E_{1,\text{QW}}$ ) and ( $E_{\text{WL}}-E_{1,\text{QW}}$ ) are responsible for the 12.7 and 10.3  $\mu\text{m}$  responses. In this case, the energy difference between the two peaks at either MWIR or LWIR ranges would correspond to the same value of ( $E_{0,\text{QW}}-E_{\text{WL}}$ ). The similar energy differences 24.4 and 22.8 meV at MWIR and LWIR ranges have confirmed the transition model.

The sample discussed in this paper is grown on (1 0 0)-oriented semi-insulating GaAs substrates by Riber Compact 21 solid-source molecular beam epitaxy system. The sample structure is shown in Table 1. With 300 and 600 nm n-type GaAs layers doped to  $2 \times 10^{18} \text{ cm}^{-3}$  as the top and bottom contact layers, the 10-period InAs/GaAs/Al<sub>0.2</sub>Ga<sub>0.8</sub>As structures were grown as the active region. For each period, 1 nm undoped GaAs/2.4 ML InAs QDs/8 nm n-type GaAs QD/QW structures are sandwiched between two 30 nm Al<sub>0.2</sub>Ga<sub>0.8</sub>As barrier layers. The doping density at the QW region is  $1 \times 10^{18} \text{ cm}^{-3}$  for the device. After mesa formation and metal evaporation,  $100 \times 100 \mu\text{m}^2$  devices were fabricated for measurements. The spectral responses were measured under an

\* Corresponding author. Address: 128 Sec. 2, Academia Road, Nankang, Taipei 11529, Taiwan. Tel.: +886 3 5744364; fax: +886 3 5745233.

E-mail address: [shihyen@gate.sinica.edu.tw](mailto:shihyen@gate.sinica.edu.tw) (S.-Y. Lin).

**Table 1**  
The wafer structure of the 10-period MMIP.

	Top contact	300 nm GaAs $n = 2 \times 10^{18} \text{ cm}^{-3}$
10×	25 nm $\text{Al}_{0.2}\text{Ga}_{0.8}\text{As}$	Undoped
	8 nm GaAs (Doping=)	$n = 1 \times 10^{18} \text{ cm}^{-3}$
	2.4 ML InAs QDs	Undoped
	1 nm GaAs	Undoped
	25 nm $\text{Al}_{0.2}\text{Ga}_{0.8}\text{As}$	Undoped
	Bottom contact	600 nm GaAs $n = 1 \times 10^{18} \text{ cm}^{-3}$
	Substrate	350 mm (1 0 0) semi-insulating GaAs

edge-coupling scheme. For this purpose, the devices were polished 45° off at one side of the samples. The infrared light was normally incident to the polished surface. The applied voltages to be positive or negative were defined according to the voltage polarity applied to the top contact. The measurement system for spectral response consists of a Spectral 100 Fourier transformation infrared (FTIR) spectroscopy coupling with a Janis cryostat and a current preamplifier. The current–voltage ( $I$ – $V$ ) characteristics were measured by using the Keithley 236 source measure unit [4–6].

The 10 K spectral responses of the device at  $\pm 2.8$  V are shown in Fig. 1a. As shown in the figure, 4.8 and 12.7  $\mu\text{m}$  responses are observed for the device under 2.8 V, while 5.3 and 10.3  $\mu\text{m}$  responses are observed under  $-2.8$  V. The results suggest that there are four different transition mechanisms involved in the spectral response measurements. The 10 K spectral responses of the device at  $\pm 2.0$  V are shown in Fig. 1b. As shown in the figure, both 4.8 and 5.3  $\mu\text{m}$  responses at MWIR range are observed for the device at lower applied voltages, while no responses are observed at the LWIR range. The results suggest that both transition mechanisms at the MWIR range would occur at the same time for the device.

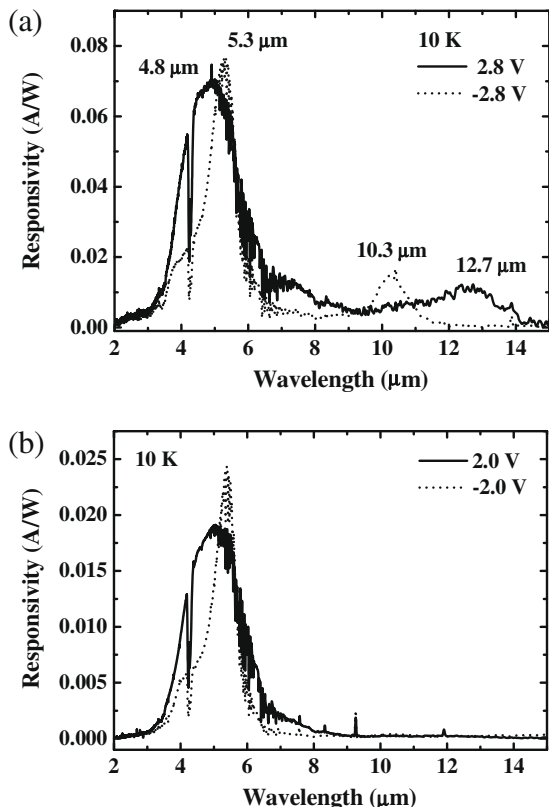


**Fig. 1.** The 10 K spectral responses of the device at (a)  $\pm 2.8$  V and (b)  $\pm 2.0$  V.

Dominant responses 4.8 and 5.3  $\mu\text{m}$  are observed at positive and negative biases, respectively. The coexistence of the two peaks at 12.7 and 10.3  $\mu\text{m}$  is not observed from the spectral responses at either  $\pm 2.8$  or  $\pm 2.0$  V. The results suggest that the transition mechanisms of the peaks at the LWIR range is different from those at the MWIR range.

To further investigate the transition mechanisms of the device, responses of the device measured under IR light irradiation with different polarizations are performed [4–5]. The measurement configuration is shown in Fig. 2a. The normalized MWIR and LWIR responsivities of the device measured under the IR light irradiation with different polarizations at 2.8 and  $-2.8$  V are shown in Fig. 2b and c, respectively. Compared with the values obtained under p-mode IR light irradiation, the MWIR/LWIR responsivities under s-mode IR light irradiation are reduced to 66/40% and 65/40% at 2.8 and  $-2.8$  V, respectively. The results suggest that although different transition mechanisms are responsible for the four peaks ob-

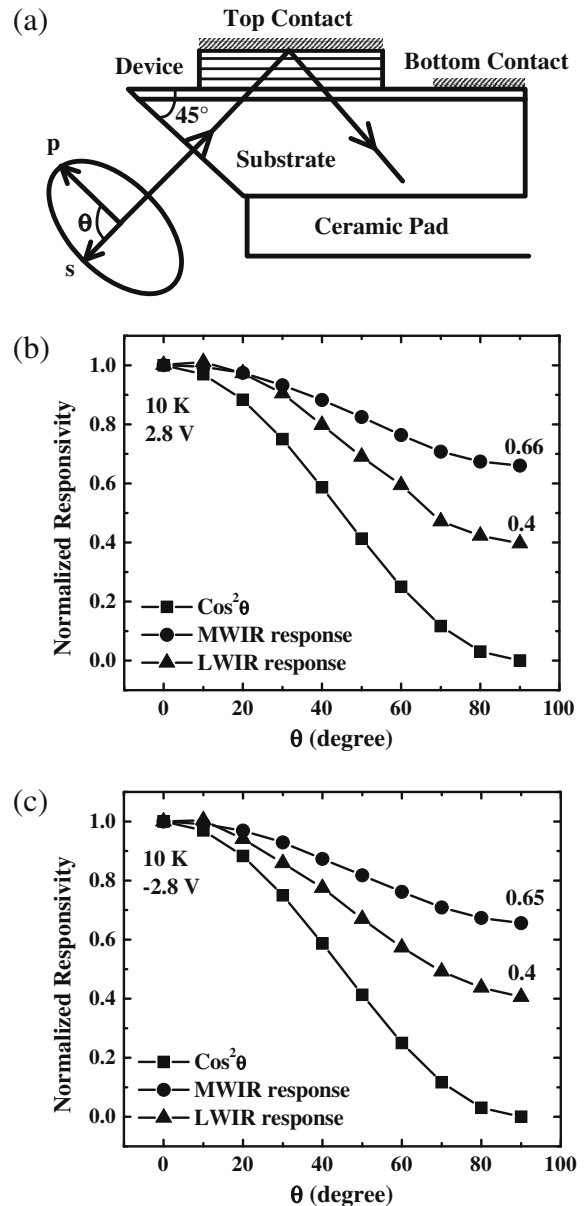


**Fig. 2.** (a) The measurement configuration of polarization-dependent responses of the device and the normalized responsivities of the device under IR light irradiation with different polarizations at (b) 2.8 and (c)  $-2.8$  V.

served at positive and negative biases, the MWIR responses at 4.8 and 5.3  $\mu\text{m}$  should be resulted from QD intra-band transitions while the LWIR responses 12.7 and 10.3  $\mu\text{m}$  from QW intra-band transitions [4]. It seems to be contradictory that both MWIR and LWIR responses would be observed for the device at the same applied voltage. The reason is that no empty states at the QD excited state would be available for electron transitions if the QW ground state is filled with electrons. In this case, it is reasonable to assume that one-electron/one-photon process is for the MWIR responses while one-electron/ two-photon process is for the LWIR responses. The observation of the LWIR responses is resulted from the re-excitation to the QW excited state of photo-excited electrons transited from the QD ground state.

To further explain the results and arguments described above, a model is proposed. A simplified schematic band diagram of the device under positive and negative biases are shown in Fig. 3. It is assumed that five states are in the structure, which are ground states and first excited states in both the QD and QW regions denoted as  $E_{0,QD}$ ,  $E_{1,QD}$ ,  $E_{0,QW}$ , and  $E_{1,QW}$ , and the wetting layer state denoted as  $E_{WL}$ . According to the observations of polarization-dependent spectral responses, the responses at 4.8 and 5.3  $\mu\text{m}$  should be resulted from the QD intra-band transitions while the 12.7 and 10.3  $\mu\text{m}$  responses from QW intra-band transitions. Assuming the  $E_{1,QD}$  is fully occupied with electrons due to the n-type doping in the QW region, transitions between  $E_{0,QD}$  and other higher-order states would be less possible due to the large energy difference in-between. Therefore, two transition mechanisms (a) and (b), as shown in Fig. 3, should be responsible for the 4.8 and 5.3  $\mu\text{m}$  responses of the device, where (a) represents the  $E_{1,QD}-E_{0,QW}$  transition and (b) the  $E_{1,QD}-E_{WL}$  transition. Due to electron wave function of  $E_{WL}$  is similar to that of  $E_{0,QW}$ , it is reasonable to assume that the normal incident absorption ratio should be similar for both transitions of (a)  $E_{1,QD}-E_{0,QW}$  and (b)  $E_{1,QD}-E_{WL}$  [8]. When an external voltage is applied to the devices, both transitions (a) and (b) would occur. However, when the device is under positive biases, as compared to the photon-excited electrons at  $E_{0,QW}$ , the phonon-assisted tran-

sition to the  $E_{0,QW}$  state would be necessary for the electrons at  $E_{WL}$  prior tunneling through the AlGaAs barrier layer. In this case, transition (a) would be dominant for the devices positively biased such that the 4.8  $\mu\text{m}$  response would be observed. For the devices negatively biased, considering the small energy difference between  $E_{0,QW}$  and  $E_{WL}$ , the tunneling probability for electrons at the two states should be similar. However, considering the smaller energy between  $E_{1,QD}$  and  $E_{WL}$ , the absorption coefficient of transition (b) should be higher than that of transition (a). In this case, transition (b) would be dominant for the devices negatively biased such that the 5.3  $\mu\text{m}$  response would be observed. Assuming that the Fermi level of the device are lower than the  $E_{WL}$  state, the observed LWIR response of the device is attributed to the two-photon absorption with  $E_{WL}$  and  $E_{0,QW}$  as the intermediate states [9]. Therefore, dominant transitions of (c)  $E_{0,QW}-E_{1,QW}$  and (d)  $E_{WL}-E_{1,QW}$  would be observed for the device at positive and negative biases, respectively. In this case, when the device is positively biased, 12.7  $\mu\text{m}$  response would be observed while 10.3  $\mu\text{m}$  response is observed at negative biases. Another evidence supporting this argument is that the energy difference between 12.7 and 10.3  $\mu\text{m}$  is 22.8 meV, which is very close to the energy difference 24.4 meV between 4.8 and 5.3  $\mu\text{m}$ . The result is consistent with the prediction of the model that the same energy state difference ( $E_{WL}-E_{1,QD}$ ) is responsible for the peak energy differences at either MWIR or LWIR ranges.

To investigate the temperature dependence of responsivities for the device, the 10 and 77 K spectral responses of the device measured at  $-2.6$  V are shown in Fig. 4. As shown in the figure, increases of responsivities at both MWIR and LWIR regions with increasing temperatures are observed for the device. The phenomenon is quite different from the invariant photocurrents of conventional QWIP or superlattice infrared photodetectors (SLIP) [10]. For the conventional QWIP devices, considering the small temperature measurement range (10–77 K), no significant change on electron capture probability in the QW region would be observed. In this case, invariant photocurrents with increasing temperatures would be observed for the device. However, for standard QDIPs, the electron capture probability in the QD structure would rapidly decrease with increasing temperatures [11]. In this case, an increase of photocurrents with increasing temperatures would be observed for the device. In the case of MMIPs, the MWIR response of the device is resulted from the QD intra-band transitions. The MWIR response of the device would increase with increasing temperature as in the case for standard QDIPs. As for the LWIR responses, an increase in the MWIR response would represent increasing electron occupancy in the intermediate states like  $E_{WL}$  and  $E_{0,QW}$ . In this case, the transition probability in the QW structure would also increase as in the case in the QD structure. The characteristic would be quite helpful for the development of

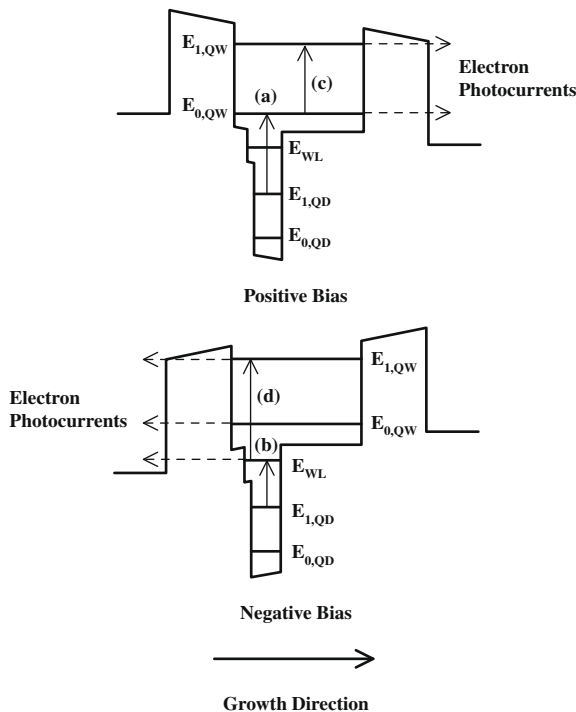


Fig. 3. A simplified schematic band diagram of the device under positive and negative biases.

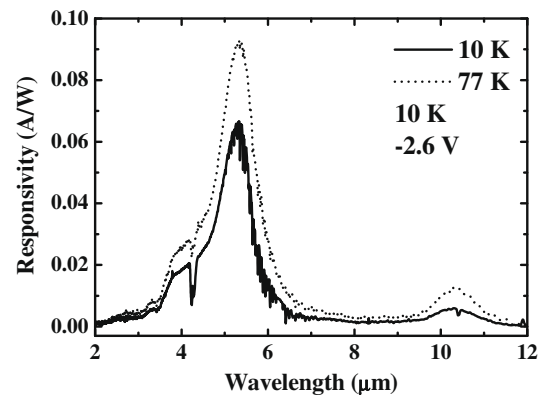


Fig. 4. The 10 and 77 K spectral responses of the device at  $-2.6$  V.

high-temperature operation infrared photodetectors in the LWIR range.

In conclusion, a 10-period QD/QW MMIP is proposed in this paper. Responses at 4.8/12.7 and 5.3/10.3  $\mu\text{m}$  at positive and negative biases are observed for the device. Compared with the peaks at MWIR range, the lower normal incident absorption of the LWIR peaks suggests that the QW intra-band transition is responsible for the responses. The QD intra-band transition should be responsible for the MWIR peaks. A model is proposed to explain the transition mechanisms of the device. While the one-photon transition process is responsible for the MWIR responses, the LWIR responses should be resulted from a two-photon process. The increases of both MWIR and LWIR responses with increasing measurement temperatures are also observed for the device. The results are different with the invariant photocurrents of QWIPs with increasing temperatures. The phenomenon is attributed to the increase of electrons in the QW ground state/wetting layer state resulted from the increase of one-photon absorption process with increasing temperatures. According to the results of this paper, multi-color detection in both the MWIR and LWIR ranges could be achieved within a single MMIP structure by properly designing the structures.

## Acknowledgements

This work was supported in part by the National Science Council, Taiwan under Grant Numbers NSC 96-2221-E-001-030 and NSC 96-2218-E-002-012.

## References

- [1] S.Y. Lin, Y.R. Tsai, S.C. Lee, *Appl. Phys. Lett.* 78 (2001) 2784–2786.
- [2] S. Chakrabarti, A.D. Stiff-Roberts, P. Bhattacharya, S. Gunapala, S. Bandara, S.B. Rafol, S.W. Kennerly, *IEEE Photon. Technol. Lett.* 16 (2004) 1361–1363.
- [3] S.F. Tang, S.Y. Lin, S.C. Lee, *Appl. Phys. Lett.* 78 (2001) 2428–2430.
- [4] S.T. Chou, M.C. Wu, S.Y. Lin, J.Y. Chi, *Appl. Phys. Lett.* 88 (2006) 173511.
- [5] S.T. Chou, C.H. Tsai, M.C. Wu, S.Y. Lin, J.Y. Chi, *IEEE Photon. Technol. Lett.* 17 (2005) 2409–2411.
- [6] S.T. Chou, S.F. Chen, S.Y. Lin, M.C. Wu, J.M. Wang, *J. Cryst. Growth* 301–302 (2007) 817–820.
- [7] S.F. Tang, C.D. Chiang, P.K. Weng, Y.T. Gau, J.J. Ruo, S.T. Yang, C.C. Shih, S.Y. Lin, S.C. Lee, *IEEE Photon. Technol. Lett.* 18 (2006) 986–988.
- [8] G. Sek, K. Ryczko, M. Motyka, J. Andrzejewski, K. Wysocka, J. Misiewicz, *J. Appl. Phys.* 101 (2007) 063539.
- [9] P. Aivaliotis, E.A. Zibik, L.R. Wilson, J.W. Cockburn, *Appl. Phys. Lett.* 92 (2008) 023501.
- [10] S.Y. Lin, Y.R. Tsai, S.C. Lee, *Jpn. J. Appl. Phys.* 40 (2001) L 1290–L 1292.
- [11] X. Lu, J. Vaillancourt, *Appl. Phys. Lett.* 91 (2007) 051115.